Dynamics of solitons of the generalized (3+1)-dimensional nonlinear Schrödinger equation with distributed coefficients*

Liu Xiao-Bei(刘晓蓓) and Li Biao(李 彪)†

Nonlinear Science Center and Department of Mathematics, Ningbo University, Ningbo 315211, *China*

(Received 11 April 2011; revised manuscript received 26 May 2011)

We present three families of soliton solutions to the generalized (3+1)-dimensional nonlinear Schrödinger equation with distributed coefficients. We investigate the dynamics of these solitons in nonlinear optics with some selected parameters. Different shapes of bright solitons, a train of bright solitons and dark solitons are observed. The obtained results may raise the possibilities of relevant experiments and potential applications.

Keywords: (3+1)-dimensional nonlinear Schödinger Equation, optical soliton, soliton propagation

PACS: 42.81.Dp, 02.30.Jr, 05.45.Yv **DOI:** 10.1088/1674-1056/20/11/114219

1. Introduction

Since the discovery of soliton by Kruskal and Zabusky,[1] there have been many significant theoretical and numerical contributions to the development of the solitons theory.[2−6] In general, a precise definition of the soliton is not easy to find. However, the soliton can be defined as a solution of a nonlinear partial differential equation (PDE) that exhibits the following properties:[6] (i) the solution should demonstrate a wave of a permanent form; (ii) the solution is localized, which means that the solution either decays exponentially to zero, such as the solitons provided by the KdV equation, or converges to a constant at infinity, such as the solitons given by the Sine–Gordon equation; (iii) the soliton interacting with other solitons preserves its character (for more detail, see page 459 and part II in Ref. [6]). With the development of the soliton theory, some powerful methods, such as the inverse scattering method,[3] the Darboux transformation,[4] the Hirota bilinear method,[5] the variational iteration method,[6] and the Adomian decomposition method,[6,7] have been proposed in the literature to examine exact solutions (especially soliton solutions) for PDEs. Recently, with the availability of symbolic computation systems, such as Mathematica and Maple, some direct methods, such as various tanh methods[8−11] and various sub-equation expansion methods,[12,13] have been developed to construct various exact solutions for some PDEs.

The nonlinear Schrödinger equation (NLSE) is one of the most useful generic mathematical models, which naturally arises in many fields of physics and attracts a great deal of attention. In the research of the standard NLSE, the concepts of bright and dark solitons are proposed for the focus and the defocus NLSEs, respectively.[3] The two definitions satisfy the strict definition of soliton. However, with the further development of the research, some types of non-travelleing wave solutions for some PDEs (especially variable-coefficients PDEs) are proposed (see Refs. [11] and [14]–[17]). Although those non-travelling wave solutions are not solitons according to the strict definition (owing to the slow changes of the wave width and the wave amplitude), the propagation is clearly soliton-like, i.e., the waves have the characteristic field profile of solitons, they are stable over a long propagation distance and under collisions, and they obey certain conservation laws. Thus, the previous authors have also labeled these solutions as bright or dark solitons. To maintain consistency, we adopt those terminologies in this paper.

Recently, various types of NLSEs including variable-coefficents and higher-dimensional NLSEs are

*Project supported by the Zhejiang Provincial Natural Science Foundations, China (Grant No. Y6090592), the National Natural Science Foundation of China (Grant Nos. 11041003 and 10735030), the Ningbo Natural Science Foundation, China (Grant Nos. 2010A610095, 2010A610103, and 2009B21003), and K.C. Wong Magna Fund in Ningbo University, China.

†Corresponding author. E-mail: biaolee2000@yahoo.com.cn

© 2011 Chinese Physical Society and IOP Publishing Ltd

attracting great attention because of their potential applications in nonlinear optics, the Bose–Einstein condensations (BECs), nonlinear quantum field theory, plasma physics, fluid mechanics, biophysics, etc. Here we cite the applications in two fields. On one hand, the optical solitons are successfully used in the long distance telecommunication, more and more attention has been paid to different versions of the NLSE that can describe the nonlinear and the dispersion management for temporal or spatial optical solitons, soliton lasers, ultrafast soliton switches in nonlinear fibres.[18] Several methods have also been developed to obtain the optical soliton solutions of various NLSEs with various nonlinearities and dispersions, and the dynamics of the excitation of the solitons were discussed.[19−25] On the other hand, based on the successful experimental realization and the theoretical analysis of the BECs in weakly interacting atomic gas,[26−29] various nonlinear excitations of the matter-wave solitons have been observed and studied.[30−35] Those studies have stimulated a large number of research activities on nonlinear optics and the BECs. In particular, very recently, great interest was focused on the (2+1)-dimensional ((2+1)D) and (3+1)-dimensional ((3+1)D) NLSEs from various viewpoints,[36−41] which provide excellent proving grounds for exploring higher-dimensional nonlinear systems with distributed coefficients.

Our interest is focused on the generalized (3+1)D NLSE with distributed coefficients[42]

$$\mathrm{i}\frac{\partial u}{\partial z}+\frac{\rho(z)}{2}\left(\frac{\partial^2 u}{\partial x^2}+\frac{\partial^2 u}{\partial y^2}+\frac{\partial^2 u}{\partial t^2}\right)+\chi(z)|u|^2u-\mathrm{i}\gamma(z)u=0, \tag{1}$$

which describes the evolution of a slowly varying wave packet envelope $u(z,x,y,t)$ in a diffractive nonlinear Kerr medium with an anomalous dispersion under the paraxial approximation. Here z is the propagation coordinate and t is the reduced time, i.e., time in the reference frame moving with the wave packet. All coordinates are made dimensionless by the choice of coefficients. The generalized NLSE is of considerable importance, as it describes the full spatiotemporal optical solitons (light bullets) in (3+1)D.[42] Functions ρ,χ and γ represent the diffraction or the dispersion, the nonlinearity and the gain/loss coefficients, respectively.

The rest of the present paper is organized as follows. In Section 2, we extend the method given in Ref. [33] to Eq. (1) and successfully present three families of exact bright and dark soliton solutions. In Section 3, we investigate the dynamics of the solitons thoroughly under some selected functions. The results presented can be applied to a variety of experimental conditions and can be used to investigate the effects of the various parameters on the formation and the propagation of the soliton. They also provide us a better physical understanding of the solitons. Finally, some conclusions are given briefly.

2. Solitons of (3+1)D NLSE with distributed coefficients

Now we extend the method given in Ref. [33] to investigate some solutions of Eq. (1) and assume these solutions as

$$u=\left[A_1+A_2\frac{\delta\cosh(\xi)+\cos(\eta)}{\cosh(\xi)+\delta\cos(\eta)}+\mathrm{i}A_3\frac{\alpha\sinh(\xi)+\beta\sin(\eta)}{\cosh(\xi)+\delta\cos(\eta)}\right]\exp(\mathrm{i}\Delta), \tag{2}$$

$$\xi=p_1x+p_2y+p_3t+g_1,$$

$$\eta=q_1x+q_2y+q_3t+g_2, \tag{3}$$

$$\Delta=h_1x^2+h_2y^2+h_3t^2+k_1x+k_2y+k_3t+g_3, \tag{4}$$

where $A_i\equiv A_i(z), h_i\equiv h_i(z)$, $p_i\equiv p_i(z), q_i\equiv q_i(z)$, $k_i\equiv k_i(z)$ and $g_i\equiv g_i(z)$ $(i=1,2,3)$ are all real functions of z to be determined, and α, β and δ are real constants.

After substituting Eq. (2) along with Eqs. (3) and (4) into Eq. (1), we first remove the exponential terms, then collect coefficients of $\sinh^i(\xi)$, $\cosh^j(\xi)$, $\sin^m(\eta)$, $\cos^n(\eta)$, x^k, y^l and t^p $(i=0,1,2,\ldots;\ j=0,1;\ m=0,1,2,\ldots;\ n=0,1;\ k=0,1,\ldots,\ l=0,1,\ldots,\ p=0,1,\ldots)$ and separate real and imaginary parts for each coefficient. We derive a set of ordinary differential equations (ODEs) with respect to A_i,h_i,k_i,g_i,p_i,q_i $(i=1,2,3)$, $\rho(z),\chi(z)$ and $\gamma(z)$. Finally, solving these ODEs, we can obtain three families of analytical solutions of Eq. (1).

Family 1

$$u_1=\Omega\left[a_0+a_1\frac{\delta\cosh(\xi)+\cos(\eta)}{\cosh(\xi)+\delta\cos(\eta)}+\mathrm{i}\frac{\alpha\sinh(\xi)+\beta\sin(\eta)}{\cosh(\xi)+\delta\cos(\eta)}\right]\exp(\mathrm{i}\Delta), \tag{5}$$

where

$$a_0=\frac{\sigma(\delta^2\beta^2+\alpha^2)}{2\sqrt{(1-\delta^2)(\beta^2+\alpha^2)}\delta},\quad a_1=\frac{\sigma\sqrt{\alpha^2+\beta^2}}{\sqrt{1-\delta^2}},$$

$$\xi=\theta(p_{10}X+p_{20}Y+p_{30}T)$$

$$+\frac{\alpha(\delta^2\beta^2-\alpha^2-2\beta^2)(p_{10}^2+p_{20}^2+p_{30}^2)}{4\sigma\delta\beta^2\sqrt{(1-\delta^2)(\alpha^2+\beta^2)}}\theta+g_{10},$$

$$\eta=\frac{\alpha\theta}{\delta\beta}(p_{10}X+p_{20}Y+p_{30}T)$$
$$+\frac{(\delta^2\beta^2-\alpha^2+2\delta^2\alpha^2)(p_{10}^2+p_{20}^2+p_{30}^2)}{4\sigma\delta^2\beta\sqrt{(1-\delta^2)(\alpha^2+\beta^2)}}\theta+g_{20},$$

$$\Delta=\theta(X^2+Y^2+T^2)$$
$$+\frac{(\delta^2\beta^2+\alpha^2)^2(p_{10}^2+p_{20}^2+p_{30}^2)}{8\beta^2\delta^2(\alpha^2+\beta^2)(\delta^2-1)}\theta+g_{30},$$

$$\theta=\frac{1}{\int_0^z 2\rho\mathrm{d}z+1},\quad \Omega=c_0\exp\left(\int_0^z\gamma\mathrm{d}z\right)\theta^{3/2},$$
$$\chi=\frac{\rho(p_{10}^2+p_{20}^2+p_{30}^2)}{\beta^2\Omega^2}\theta^2,$$
$$X=x+\frac{k_{10}}{2},\quad Y=y+\frac{k_{20}}{2},\quad T=t+\frac{k_{30}}{2},\quad (6)$$

and $\sigma=\pm1$, $\{c_0,\alpha,\beta\neq0,\delta\neq0\}$ and $\{p_{i0},k_{i0},g_{i0}\}$ $(i=1,2,3)$ are arbitrary real constants.

Family 2

$$u_2=\Omega\left[A_\mathrm{c}+A_\mathrm{s}\frac{-2A_\mathrm{s}\cosh(\xi)+2A_\mathrm{c}\cos(\eta)+\mathrm{i}\sigma\sqrt{4A_\mathrm{c}^2-A_\mathrm{s}^2}\sinh(\xi)}{2A_\mathrm{c}\cosh(\xi)-A_\mathrm{s}\cos(\eta)}\right]\exp(\mathrm{i}\Delta),\quad (7)$$

where

$$\xi=\frac{\sigma A_\mathrm{s}(q_{10}^2+q_{20}^2+q_{30}^2)}{4\sqrt{4A_\mathrm{c}^2-A_\mathrm{s}^2}}\theta+g_{10},$$
$$\eta=\theta(q_{10}X+q_{20}Y+q_{30}T)+g_{20},$$
$$\Delta=\theta(X^2+Y^2+T^2)-\frac{A_\mathrm{c}^2(q_{10}^2+q_{20}^2+q_{30}^2)}{2(4A_\mathrm{c}^2-A_\mathrm{s}^2)}\theta+g_{30},$$
$$\chi=\frac{\rho(q_{10}^2+q_{20}^2+q_{30}^2)}{(4A_\mathrm{c}^2-A_\mathrm{s}^2)\Omega^2}\theta,\quad (8)$$

and $4A_\mathrm{c}^2>A_\mathrm{s}^2$, $\Omega,\theta,\sigma,X,Y,T$ are determined by Eq. (6), $\{A_\mathrm{c},A_\mathrm{s},\ g_{i0},q_{i0}\ (i=1,2,3)\}$ are arbitrary real constants.

Family 3

$$u_3=\Omega[A_\mathrm{c}+\mathrm{i}A_\mathrm{s}\tanh(\xi)]\exp(\mathrm{i}\Delta),\quad (9)$$

where

$$\Delta=\theta(X^2+Y^2+T^2)$$
$$+\frac{1}{2}\left(1+\frac{A_\mathrm{c}^2}{A_\mathrm{s}^2}\right)(p_{10}^2+p_{20}^2+p_{30}^2)\theta+g_{30},$$
$$\xi=\theta(p_{10}X+p_{20}Y+p_{30}T)$$
$$-\frac{A_\mathrm{c}}{2A_\mathrm{s}}(p_{10}^2+p_{20}^2+p_{30}^2)\theta+g_{10},$$
$$\chi=-\frac{\rho\theta}{A_\mathrm{s}^2\Omega^2}\sum_{i=1}^{3}p_{i0}^2,\quad (10)$$

and Ω,θ,t,x,Y,T are determined by Eq. (6), $\{A_\mathrm{s}\neq0,A_\mathrm{c},g_{10},g_{30},p_{10},p_{20},p_{30}\}$ are arbitrary real constants.

To our knowledge, solutions (5), (7), and (9) are new general solutions of Eq. (1), which can describe the dynamics of the solitons in the generalized (3+1)D NLSE with distributed coefficients. From Eq. (6), we can see the chirp function, $\theta=1/(\int_0^z 2\rho\mathrm{d}z+1)$, in solutions (5), (7) and (9) is related only to the diffraction or the dispersion coefficient ρ. The chirp function can also influence the form of the solution amplitudes through the dependence of $\{\Omega,\xi,\eta\}$. At the same time, we can see that there are two arbitrary functions among functions χ, ρ and γ, so we can manage these solitons to interpret some interesting physical phenomena by selecting these arbitrary constants and arbitrary functions appropriately.

3. Dynamics of solitons of the generalized (3+1)D NLSE

In this section, we will investigate the dynamics for solutions (5), (7), and (9), respectively.

3.1. Dynamics of bright solitons in (3+1)D NLSE

In order to investigate the bright soliton (Eq. (5)), we further set $\alpha=0$ and redefine various parameters, then u_1 reduces to

$$u_{11}=\Omega_1\left[A_\mathrm{c}+A_\mathrm{s}\frac{-2A_\mathrm{c}\cosh(\xi)+A_\mathrm{s}\cos(\eta)+\mathrm{i}\sigma\sqrt{A_\mathrm{s}^2-4A_\mathrm{c}^2}\sin(\eta)}{A_\mathrm{s}\cosh(\xi)-2A_\mathrm{c}\ \cos(\eta)}\right]\exp(\mathrm{i}\Delta),\quad (11)$$

where A_c and A_s are arbitrary real constants with $A_s^2 > 4A_c^2$ and

$$\begin{aligned}
\Delta &= \theta(X^2+Y^2+T^2) \\
&\quad - \frac{A_c^2(p_{10}^2+p_{20}^2+p_{30}^2)}{2(A_s^2-4A_c^2)}\theta + g_{30}, \\
\xi &= \theta(p_{10}X+p_{20}Y+p_{30}T)+g_{10}, \\
\eta &= \frac{\sigma A_s(p_{10}^2+p_{20}^2+p_{30}^2)}{4\sqrt{A_s^2-4A_c^2}}\theta + g_{20}, \\
\Omega_1 &= \exp\left(\int_0^z \gamma \mathrm{d}z\right)\theta^{3/2}, \\
\chi &= \frac{\rho(p_{10}^2+p_{20}^2+p_{30}^2)}{(A_s^2-4A_c^2)\Omega_1^2}\theta. \qquad (12)
\end{aligned}$$

When soliton amplitude A_s vanishes, u_{11} reduces to the continuous wave solution $u_c = A_c\Omega\exp(\mathrm{i}\Delta)$ with the loss/gain and the frequency chirp. When continuous wave amplitude A_c vanishes, u_{11} reduces to the bright soliton $u_s = A_s\Omega\mathrm{sech}(\xi)\exp[\mathrm{i}(\Delta+\eta)]$, where $\Delta+\eta = \theta(X^2+Y^2+T^2)+\sigma(p_{10}^2+p_{20}^2+p_{30}^2)\theta/4+g_{30}$. Thus, u_{11} represents a bright soliton embedded in a continuous wave light background. At the same time, when $A_c \ll A_s$, the background is small within the existence of the bright soliton.

In order to understand the significance of the solutions in Families 1–3, we can investigate their features by using computer simulations. For simplicity, we consider only two types of functions of θ to illustrate the features of the solutions.

Figures 1(a) and 1(b) show the evolution of the amplitude profile of solution (11), presented as a function of $V = p_{10}X + p_{20}Y + p_{30}T$ and z for frequency chirp parameter $\theta = \sin(0.4z)^2$ and different gain/loss coefficient γ. As we can see from Fig. 1, solution (11) represents a bright pulse that propagates on a continuous wave background with the loss/gain and the frequency chirp. The main characteristic of the propagation is the peak changing property of the field amplitude, i.e., the pulse has a decrease in peak value, a broadening in width and an increase in peak spacing as the pulse propagates along the inhomogeneous fibre for $\gamma < 0$, while they are the opposite for $\gamma > 0$.

Figures 2(a) and 2(b) show the evolution of the amplitude profile of solution (11), presented as a function of $V = p_{10}X + p_{20}Y + p_{30}T$ and z for frequency chirp parameter $\theta = [\exp(0.0001z)+\exp(-0.1z)]^{-0.5}$ and different values of gain/loss coefficient γ. From Fig. 2, we can see that firstly, the amplitude of bright soliton u_{11} increases rapidly to a maximum, then decays to the background very slowly. At the same time, we can see that when $\gamma > 0$, the velocity of dissipation is lower than that when $\gamma < 0$.

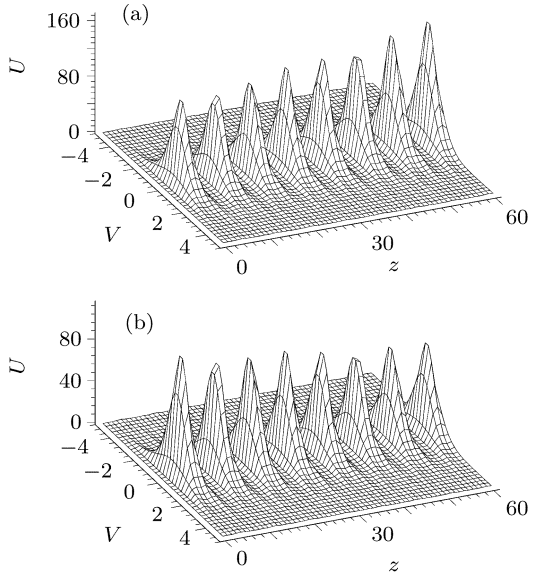


Fig. 1. Evolution plots of intensity $U = |u_{11}|^2$, presented each as a function of $V = p_{10}X + p_{20}Y + p_{30}T$ and z. Input parameters are $A_c = 1, A_s = 10, p_{10} = 0.2, p_{20} = 0.3, p_{30} = 0.4, g_{10} = g_{20} = 0, \theta = \sin^2(0.4z)$. In panel (a), $\gamma = 0.003$ and in panel (b), $\gamma = -0.003$.

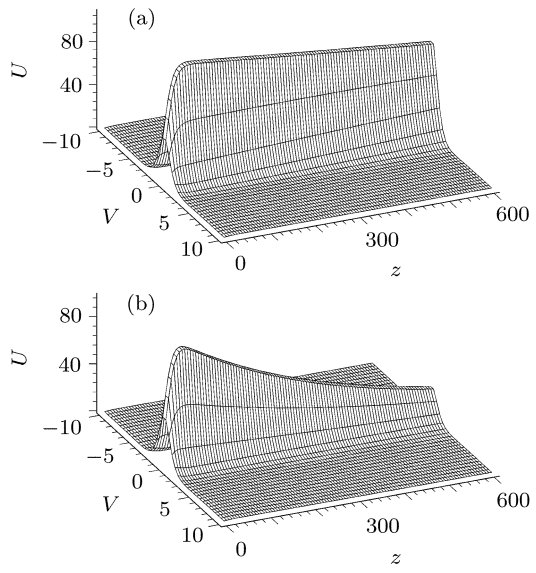


Fig. 2. Evolution plots of intensity $U = |u_{11}|^2$, presented each as a function of $V = p_{10}X + p_{20}Y + p_{30}T$ and z. Input parameters are $A_c = 1, A_s = 10, p_{10} = 0.2, p_{20} = 0.3, p_{30} = 0.4, g_{10} = g_{20} = 0, \theta = [\exp(0.0001z) + \exp(-0.1z)]^{-0.5}$. In panel (a), $\gamma = 0.005$ and in panel (b), $\gamma = -0.005$.

Furthermore, we find that when $\cosh(\xi) = -2A_c\cos(\eta)/A_s + A_s/[A_c\cos(\eta)]$ $(\sinh(\xi) = 0)$, the intensity of soliton (11) arrives at the minimum (maxi-

mum) expressed as

$$|u_{11}|^2_{\min} = A_c^2\left[1-\frac{(A_s^2-4A_c^2)\cos^2(\eta)}{A_s^2-4A_c^2\cos^2(\eta)}\right] \times \exp\left(\int_0^z 2\gamma \mathrm{d}z\right)\theta^3,$$
$$|u_{11}|^2_{\max} = \left[A_c^2+\frac{A_s(A_s^2-4A_c^2)}{A_s-2A_c\cos(\eta)}\right] \times \exp\left(\int_0^z 2\gamma \mathrm{d}z\right)\theta^3. \quad (13)$$

This means that bright soliton (11) can propagate only between the minimum and the maximum values. Figure 3 shows the evolution plots of the maximal and the minimal intensities given by $|u_{11}|^2_{\max}/100$ (dotted line) and $100|u_{11}|^2_{\min}$ (dashed line), respectively, and the background intensity (solid line) with different parameters. According to Fig. 3, with the time evolution, the intensities of the maximal, the background and the minimal intensities are either increase or decrease simultaneously.

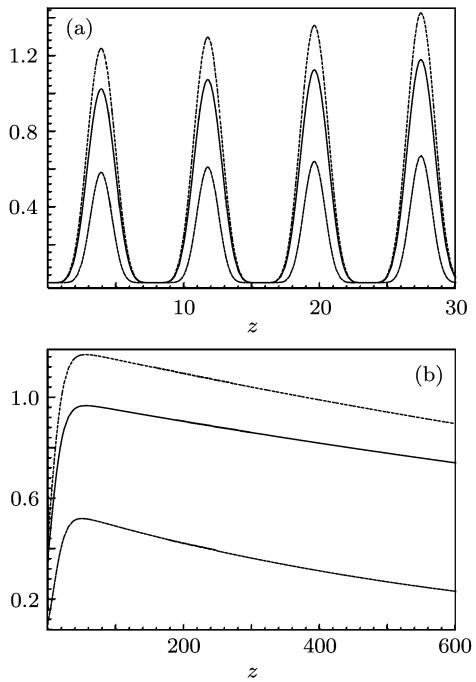


Fig. 3. Evolution plots of the maximal ($|u_{11}|^2/100$) and the minimal ($100|u_{11}|^2$) (dotted line and dashed line) and the continuous wave background ($|u_c|^2$) intensities (solid line) along the propagation direction of fibre. The parameters in panel (a) are the same as those in Fig. 1(a) and the parameters in panel (b) are the same as those in Fig. 2(a).

Now we investigate bright soliton (7). An analysis reveals that solution u_2 is periodic with period $L = 2\pi/\theta$ in the normalized temporal coordinate $V = q_{10}X + q_{20}Y + q_{30}T$ and aperiodic with respect to z. Note that period L is not a constant due to the presence of function θ. Figure 4 shows the evolution of the amplitude profile of u_2, presented as a function of $V = q_{10}X + q_{20}Y + q_{30}T$ and z for different frequency chirp parameters and the same gain coefficient $\gamma = 0.003$. From Fig. 4, we can see that in spite of $\theta = \sin^2(0.2z)^2$ or $\theta = [\exp(0.0001z) + \exp(-0.1z)]^{-0.5}$, the plots present a periodic property in the direction of the normalized temporal coordinate V. In the direction of space variable z, the amplitude in Fig. 4(a) increases periodically and that in Fig. 4(b) firstly increases rapidly to a maximum, then decays to the background slowly.

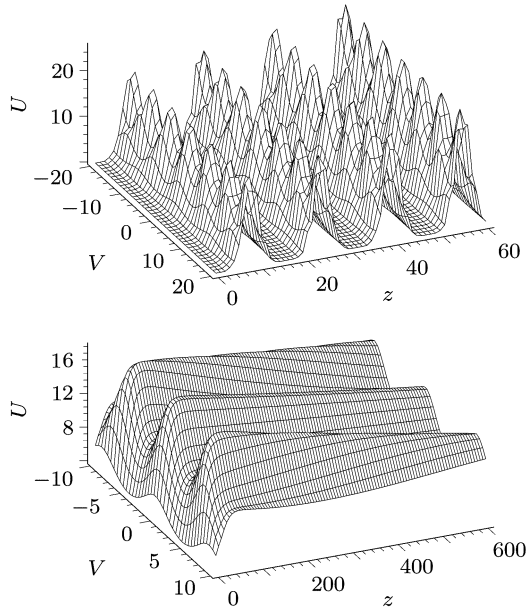


Fig. 4. Evolution plots of intensity $U = |u_2|^2$, presented each as a function of $V = q_{10}X + q_{20}Y + q_{30}T$ and z. Input parameters are $A_c = 4, A_s = 1, q_{10} = 0.2, q_{20} = 0.3, q_{30} = 0.4, g_{10} = g_{20} = 0, \gamma = 0.003$. In panel (a), $\theta = \sin^2(0.2z)$ and in panel (b), $\theta = [\exp(0.0001z) + \exp(-0.1z)]^{-0.5}$.

Thus from Fig. 4, we can see that when γ is taken to be the same small positive parameter, besides the periodic property in the direction of V, the amplitudes of u_2 present different evolution patterns under different θ values along the optical fibre. At the same time, when γ is taken to be a small negative parameter, the evolution of u_2 also demonstrates periodic properties in the direction of V regardless of the amplitude of u_2 increasing or decreasing. Therefore, the solution with similar u_2 is usually considered as a modulation instability process in the inhomogeneous fibre medium.[3,19] In application, the modulation instability can be used to produce a train of optical solitons similar to the solitons in Fig. 4 obtained by the numerical simulation. It may be useful for producing a train of compressible optical solitons.

3.2. Dynamics of a dark soliton in (3+1)D NLSE

In the following, we investigate the dynamics of dark soliton (8). From Eq. (8), we can obtain the intensity of the background as

$$|u_{3c}|^2 = (a_1^2 + \alpha^2)c_0^2 \exp\left(\int_0^z 2\gamma \mathrm{d}z\right)\theta^3. \qquad (14)$$

According to Eq. (13), the intensity of the background is determined mainly by functions γ and θ. Figures 4(a) and 4(b) show the evolution of the amplitude profile of solution (8), presented as a function of $V = p_{10}X + p_{20}Y + p_{30}T$ and z for different frequency chirp parameters and the same gain coefficient. As shown in Fig. 5(a), solution (10) represents a dark pulse that propagates along the inhomogeneous fibre with the gain and frequency chirp $\theta = \sin^2(0.4z)$. The main characteristic of the propagation is the peak changing property of the field amplitude, i.e., the pulse has a increase in peak value, a broadening in width and an increase in peak spacing. From Fig. 5(b), we can see that first the amplitude of dark soliton u_3 increases rapidly to a maximum, then decays to the background very slowly. When the amplitude of the dard soliton decreases, the soliton broadens.

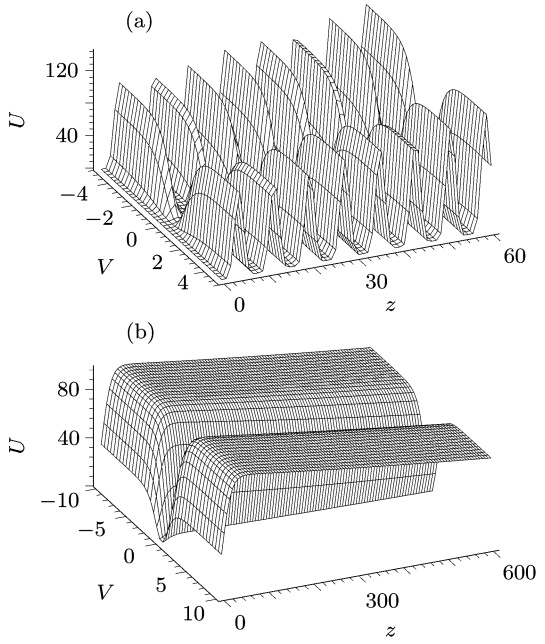


Fig. 5. Evolution plots of intensity $U = |u_3|^2$, presented each as a function of $V = p_{10}X + p_{20}Y + p_{30}T$ and z. The parameters in panels (a) and (b) are the same as those in Figs. 1(a) and 2(a), respectively.

4. Conclusion and discussion

In this paper, we present three families of soliton solutions to the generalized (3+1)-dimensional nonlinear Schrödinger equation with the diffraction or the dispersion, the nonlinearity and the gain/loss coefficients. We investigate the dynamics of these solitons in nonlinear optics with some selected parameters and discuss the influence of the frequency chirping parameter and the gain/loss parameter in detail. From the analysis and the plots, we can see that the bright and the dark solitons undergo decreasing or increasing depending on the signs of the gain/loss parameters. Particularly, a family of bright solitons can be used to describe the modulation instability in the inhomogeneous fibre medium and produce a train of compressible optical solitons. The obtained results can also be applied to other physical fields, such as the Bose–Einstein condensate and plasma physics, and open up opportunities for further study on the related experiments.

References

[1] Zabusky N J and Kruskal M D 1965 *Phys. Rev. Lett.* **15** 240

[2] Drazin P G and Johnson R S 1996 *Solitons: an Introduction* (Cambridge: Cambridge University Press)

[3] Ablowitz M J and Clarkson P A 1991 *Soliton, Nonlinear Evolution Equations and Inverse Scattering* (New York: Cambridge University Press)

[4] Gu C H, Hu H S and Zhou Z X 1999 *Darboux Transformation in Soliton Theory and Its Geometric Applications* (Shanghai: Shanghai Scientific and Technical Press) (in Chinese)

[5] Hirota R 2004 *The Direct Method in Soliton Theory* (Cambridge: Cambridge University Press)

[6] Wazwaz A M 2009 *Partial Differential Equations and Solitary Waves Theory* (Springer: High Education Press)

[7] Adomian G 1994 *Solving Frontier Problems of Physics: The Decomposition Method* (Boston: Kluwer Academic Publishers)

[8] Li Z B and Liu Y P 2002 *Comput. Phys. Commun.* **148** 256

[9] Fan E 2000 *Phys. Lett.* A **277** 212

[10] Li B, Chen Y and Zhang H Q 2002 *J. Phys.* A **35** 8253

[11] Gao Y T and Tian B 2001 *Comput. Phys. Commun.* **133** 158

[12] Fan E G 2003 *J. Phys.* A **36** 7009

[13] Li B, Chen Y and Li Y Q 2008 *Z. Naturforsch.* **63a** 763

[14] Serkin V and Hasegawa A 2000 *Phys. Rev. Lett.* **85** 4502

[15] Ponomarenko S A and Agrawal G P 2006 *Phys. Rev. Lett.* **97** 013901

[16] Serkin V N, Hasegawa A and Belyaeva T L 2007 *Phys. Rev. Lett.* **98** 074102

[17] Wang J, Li B and Ye W C 2010 *Commun. Theor. Phys.* **53** 698

[18] Hasegawa A and Kodama Y 1995 *Solitons in Optical Communications* (Oxford: Oxford University Press)

[19] Li L, Li Z H, Li S Q and Zhou G S 2004 *Opt. Commun.* **234** 169

[20] Li Z D, Li Q Y, He P B, Bai Z G and Sun Y B 2007 *Ann. Phys.* **322** 2945

[21] Zhang H P, Li B and Chen Y 2010 *Chin. Phys.* B **19** 060302

[22] Li B 2007 *Int. J. Mod. Phys.* C **18** 1187

[23] Li H M, Li Y S and Lin J 2009 *Chin. Phys.* B **18** 3657

[24] Wang H and Li B 2011 *Chin. Phys.* B **20** 040203

[25] Zhang H P, Li B, Chen Y and Huang F 2010 *Chin. Phys.* B **19** 020201

[26] Anderson M H, Ensher J R, Matthews M R, Wieman C E and Cornell E A 1995 *Science* **269** 198

[27] Bradley C C, Sackett C A, Tollett J J and Hulet R G 1995 *Phys. Rev. Lett.* **75** 1687

[28] Davis K B, Mewes M O, Andrews M R, van Druten N J, Durfee D S, Kurn D M and Ketterle W 1995 *Phys. Rev. Lett.* **75** 3969

[29] Dalfovo F, Giorgini F, Pitaevskii L P and Stringari S 1999 *Rev. Mod. Phys.* **71** 463

[30] Lü B B, Hao X and Tian Q 2011 *Chin. Phys.* B **20** 020308

[31] Wang Z X, Ni Z G, Cong F Z, Liu X S and Chen L 2010 *Chin. Phys.* B **19** 113205

[32] Wang B, Tan L, Lü C H and Tan W T 2010 *Chin. Phys.* B **19** 117402

[33] Li B, Zhang X F, Li Y Q, Chen Y and Liu W M 2008 *Phys. Rev.* A **78** 023608

[34] Qi R, Yu X L, Li Z B and Liu W M 2009 *Phys. Rev. Lett.* **102** 185301

[35] Hu X H, Zhang X F, Zhao D, Luo H G and Liu W M 2009 *Phys. Rev.* A **79** 023619

[36] Wu L, Li L, Zhang J F, Mihalache D, Malomed B A and Liu W M 2010 *Phys. Rev.* A **81** 061805(R)

[37] Hu X and Li B 2011 *Chin. Phys.* B **20** 050315

[38] Yan Z Y and Konotop V V 2009 *Phys. Rev.* E **80** 036607

[39] Yan Z Y and Hang C 2009 *Phys. Rev.* A **80** 063626

[40] Gao Y and Lou S Y 2009 *Commun. Thoer. Phys.* **52** 1031

[41] Zheng L and Tang Y 2010 *Chin. Phys.* B **19** 044209

[42] Belic M, Nikola P, Zhong W P, Xie R H and Chen G 2008 *Phys. Rev. Lett.* **101** 123904